ECE 445

SENIOR DESIGN LABORATORY

FINAL REPORT (DRAFT)

# Customizable Automatic Pottery Wheel-Throwing Machine

**Team #22**

MOFEI LI (mofeili2@illinois.edu)
SHIHAN LIN (shihan3@illinois.edu)
MINHAO SHI (minhaos3@illinois.edu)
ZIXU ZHU (zixuzhu2@illinois.edu)

TA: TAOCHENG YU

May 18, 2025

# Abstract

Traditional pottery wheel throwing requires skilled craftsmanship to achieve precision in shape, symmetry, and wall thickness, which places high demands on amateurs to realize their thoughts. This project presented a new solution, the Customizable Automatic Pottery Wheel-Throwing Machine. The machine offers an intuitive graphical UI for pottery shaping, lowering the barrier for starters to express their own ideas. It supports full automation on the critical opening, pulling up, and shaping steps of pottery manufacturing based on user input at a graphical UI. Our system includes a robotic manipulator based on the SCARA kit, a standalone pottery wheel, an integrated software controller, and a custom PCB motor driver. In this report, we include design details, cost, schedules, technical requirements, and verifications of our design.

# Contents

# 1 Introduction

## 1.1 Purpose

The traditional wheel-throwing method for pottery demands high craftsmanship for consistent results. For those who are interested in pottery, their ideas might be unrealizable due to the long cycle of study to master basic skills. To help solve this problem, we have implemented a machine to assist the design and production of pottery, capable of implementing customized shapes with higher accuracy and efficiency.

A complete pottery-forming process consists of five steps, id est, centering, opening, pulling up, shaping, and cutting off. We mainly focus on the opening, pulling up, and shaping, which are the most significant steps for the final results.

## 1.2 Functionality

- **Automated Shaping**: The manipulator based on the SCARA kit implements the centering, opening, pulling up and shaping.
- **Customizable parameters**: Users can use a graphical interface to precisely control the parameters of the clay, including the shape of the clay and the thickness of the walls. And the driver can control the robot arm to shape the clay correctly according to the parameters.

## 1.3 Subsystem Overview

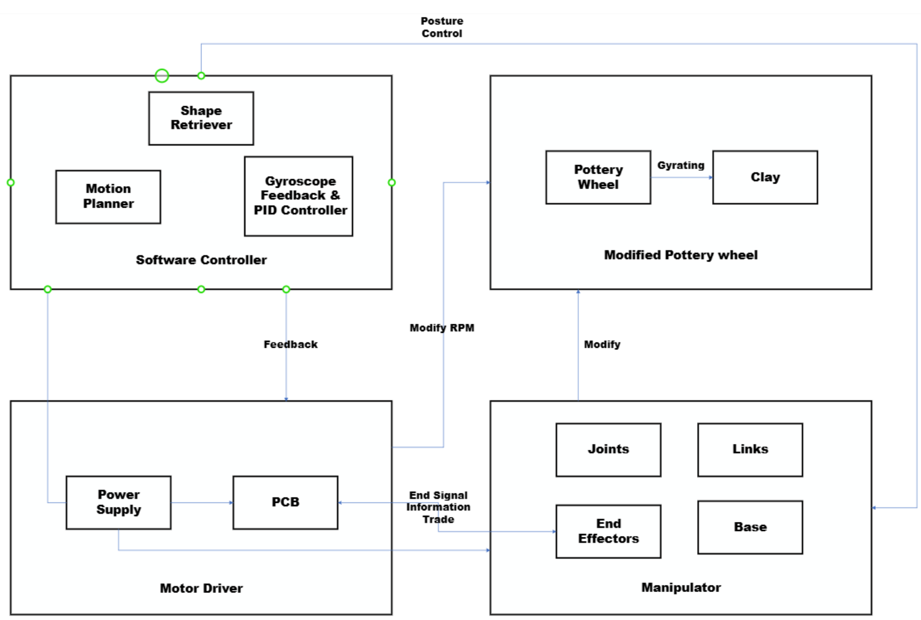


Figure 1: Block Diagram

- **Manipulator**: 5-link robot arm based on the SCARA kit, driven by three motors and two servos , it can move freely in three dimensions. The specially designed end effector can easily shape the clay.
- **Motor Driver**: A PCB board using a microcontroller (ATSAMD21) to drive motors and a WIFI module (ESP8266MOD chip) to connect with the host computer. Three NEMA 17 stepper motors with motor driver module A4988 to drive the SCARA-kit-based robot arm. One SG90/MG90S servo motor to drive the wrist and one MG995/DS3218 to drive the gripper.
- **Software Controller**: The hardware driver is completed using Arduino IDE and burned into the motor drive. The upper program uses the Python language to create a controllable graphical interface and convert user requirements into executable parameters and send them to the motor drive.
- **Pottery Wheel**: The pottery wheel with adjustable RPM (0-240) which is necessay for clay shaping.

# 2 Design

## 2.1 Manipulator

### 2.1.1 Skeleton based on the SCARA kit

The major challenge in hardware design is the form of the manipulator. To achieve our goal, the manipulator should have a minimum workspace as shown in Figure 2; in other words, it should have at least two translational degrees of freedom (DoF).

Initially, we came up with a layout that involves two lead screws, as shown in Figure 3, the vertical screw is mounted on the horizontal one, controlling the axial and radial movement in the workspace, respectively. However, this device occupies a large amount of space, especially in the radial direction of the pottery wheel. Similar designs also face some problems; for example, if we move the horizontal screw off the radial direction, there would be challenges in connecting and supporting the vertical one, and if we separate the vertical and horizontal screws and mount the pottery wheel on top of the horizontal one instead, the weight of the wheel could be a serious issue to consider.

Then, inspired by the Selective Compliance Assembly Robot Arm (SCARA) model, we adapt an open-source 3D-printed SCARA kit from jjrobots [1] as our basic skeleton. Figure 4 shows the SCARA layout we use in the subsequent development. It has a prismatic joint and three revolute joints, where the revolute joints take the place of the horizontal screw. While the first two control the reach, the last revolute joint aligns the end-effector plane back with the workspace. The higher DoF also enables more complex operations.

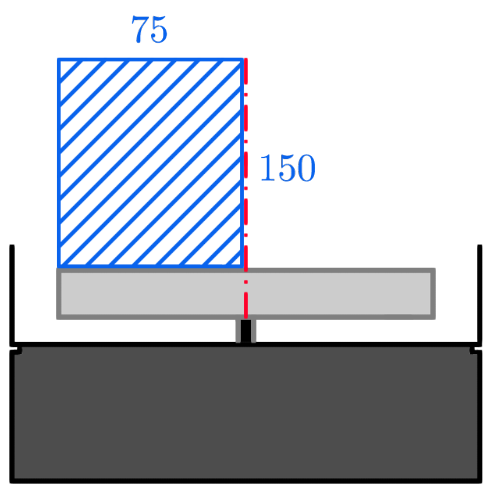


Figure 2: Minimum Workspace of Manipulator (Unit: mm).

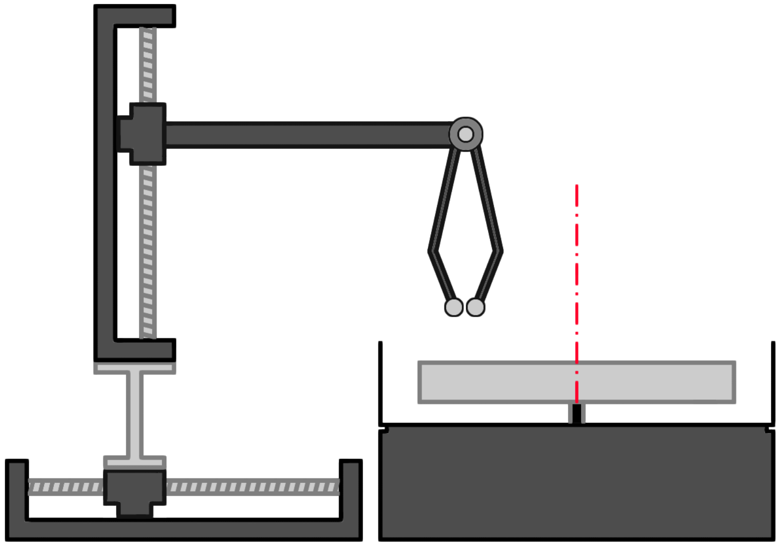

Figure 3: The Initial Dual Lead Screw Layout. The radial size of the device is quite large, leading to a non-optimal space occupation.

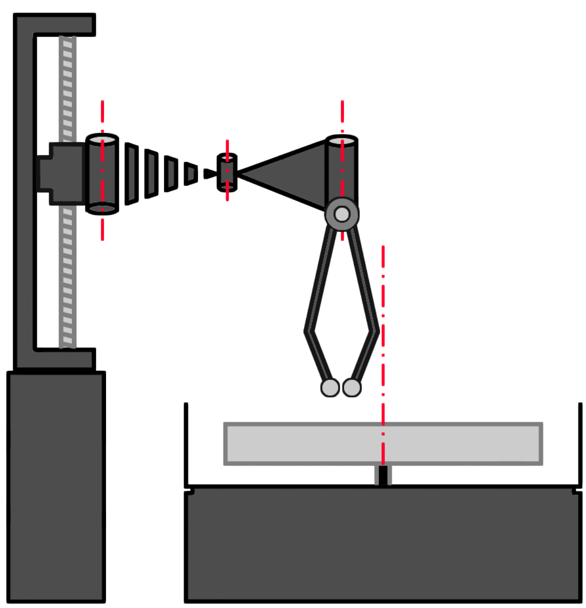

Figure 4: The SCARA Layout. Compared to the dual screw layout, it is more compact and powerful.

### 2.1.2 Gripper Jaws & Adapter

With the skeleton based on the SCARA kit, we are able to position the manipulator in space. However, the pre-shaped adobe and the final pottery have a maximum height of approximately 10 cm. This requires us to design and model a dedicated gripper with a length over 10 cm to avoid potential collisions.

First, we have considered the parallel link structure, as shown in Figure 5, to transmit the torque to the end effectors. However, after a careful evaluation, we agree that this structure is hard to implement due to its high requirement for material strength and inconvenient to calculate due to the non-linear motion of the end effectors.

Instead, we select an integrated structure for the gripper. As shown in Figure 6, this gripper increases the distance between the servo output shaft and the end effectors to approximately 120 mm, effectively preventing collisions. In this case, the end effectors will have different contact points lying on a circle, so that the most ideal end effectors should be in a spherical structure.

Since the output torque of the SG90 servo is quite limited (1.6 kgf·cm), we substitute it with the MG995 servo with a maximum torque of 13 kgf·cm or the DS3218 servo of 20 kgf·cm. To mount the larger servo on the gripper, we also design a new gripper adapter, as shown in Figure 7; the gripper jaws also need a pair of larger gears to adapt to the new output transmission plate and the new spacing of the jaw axes, as shown in Figure 8. The overall design has one prismatic joint driven by the stepper motor, two revolute joints by the same type of stepper motors, and two more revolute joints by servos.

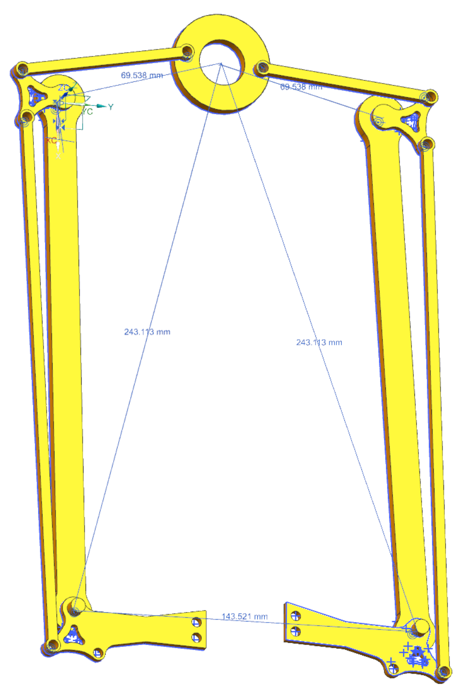


Figure 5: Draft of the Parallel Link Structure.

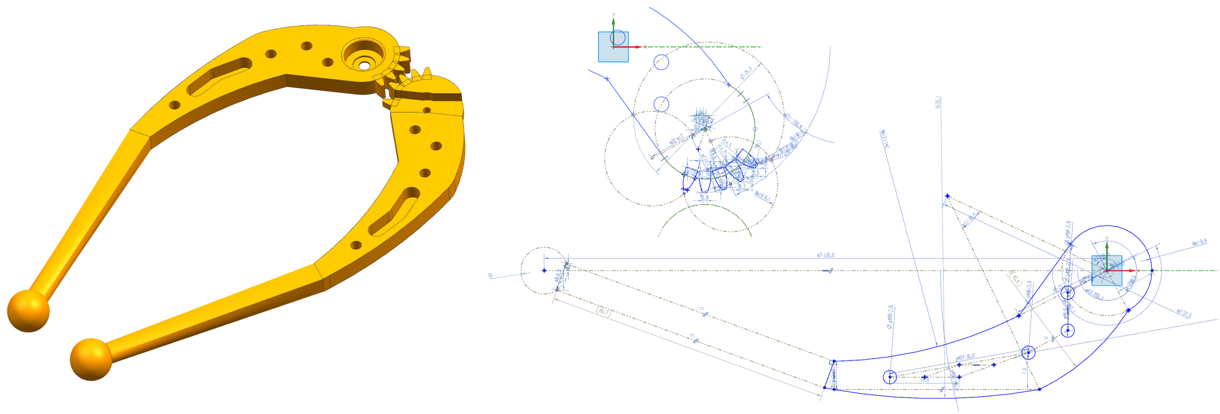

Figure 6: Gripper Jaws Driven by SG90 Servo with Main Cross Section.

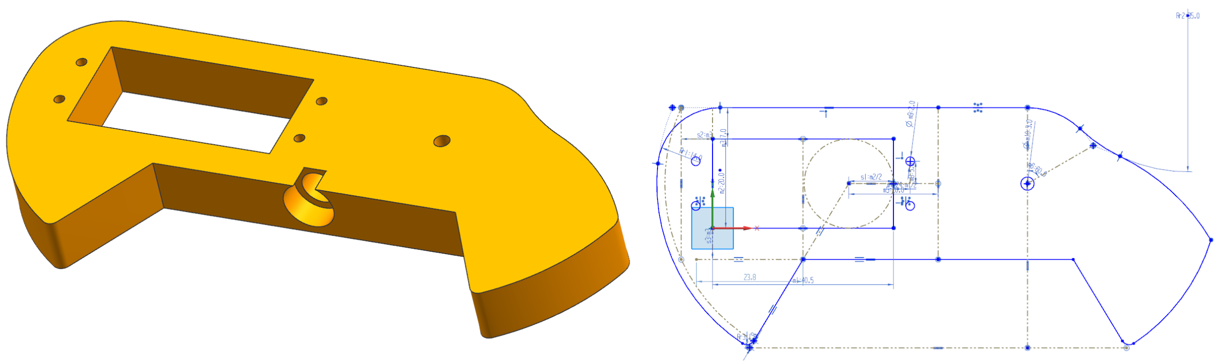

Figure 7: Gripper Adapter for MG995 Servo with Main Cross Section.

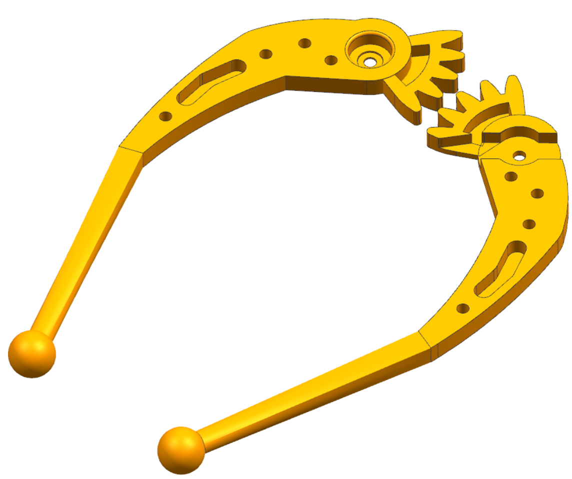

Figure 8: Gripper Jaws Driven by MG995 Servo. The gears are magnified to adapt to the MG995 output transmission plate.

## 2.2 Motor Driver

### 2.2.1 Power Supply

The pottery wheel is driven directly by a 220V AC household power supply, as shown in Figure 9. For manipulators, stepper motors are controlled by pulse signals generated by PCBs, which require a power adapter. As shown in the figure below, the adapter can accept 100-240V AC and then convert it to 12V DC theoretically. This 12V voltage is mainly used to power 2 stepper motors. Meanwhile, we power on the PCB board mainly using the VBUS pin of a MICRO USB 5S port.


Figure 9: Integrated PCB and AC/DC Adaptor

### 2.2.2 PCB

The PCB board serves as the core component of this integrated system, seamlessly bridging hardware control and software communication. It precisely manages multiple stepper motors through dedicated driver circuits that convert digital commands into accurate pulse signals while implementing essential protection mechanisms. During the simulation, the board processes real-time data from various sensors, conditioning these signals for a reliable software interpretation. We optimized and customized the PCB board based on the SCARA kit. We adjust the composition of circuit elements, cut out the parts we do not need, and update some chip versions. The paragraphs following each figure provide detailed descriptions of the individual PCBs.

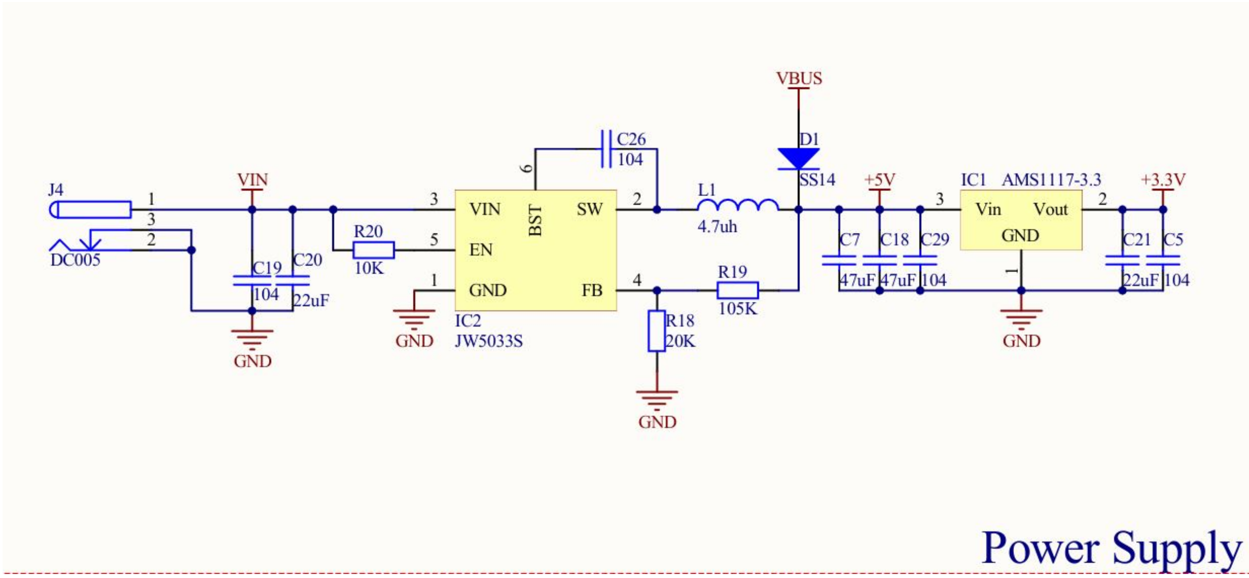


Figure 10: PCB Schematics of Power Supply

The power supply part get power both from the J4 pin and the VBUS pin of the MICRO USB 5S port in Figure 11 connected to the computer. The power system uses a three-stage conversion design. First, in Figure 10, the DC005 connector provides 12V/2A input power. Then, the JW5033S buck converter steps this down to 5V. Finally, the AMS1117-3.3 regulator converts the 5V to a stable 3.3V output. This step-down approach ensures stable power while reducing overall consumption. The JW5033S operates at a 500 kHz switching frequency. It works with a 4.7 $\mu$H inductor to efficiently convert 12V to 5V. The conversion typically achieves 92 percent efficiency. The AMS1117-3.3 takes the 5V input and outputs 3.3V for the MCU and digital circuits. It requires at least 4.4V input voltage to work properly. The JW5033S's 5V output meets this requirement perfectly.

The Micro USB 5S connector's VBUS pin supplies 5V power. This powers two servo motors with low current. It also provides power for other circuit modules.

The control of two servo motors and three NEMA 17 stepper motors is implemented through the ATSAMD21G18A-AU microcontroller, along with real-time sensor data acquisition and bidirectional communication with computer programs. The servo models include SG90/MG90S and MG995/DS3218. These two sets of servo motors operate at voltages of 4.8V-6V and 6V-8.4V, respectively, featuring torque ranges from 1.3 kg·cm to 20 kg·cm with different response speeds and operational characteristics, though all utilize standard 50Hz PWM control signals with 0.5-2.5ms pulse width modulation. [2] For wrists we use SG90 or MG90S since they do not need a high torque range, while for grippers we use MG995 or DS3218 with a torque range from 13 kg·cm to 20 kg·cm to provide extra force for clamping. The servos connect to the chip's PA08 and PA09 pins in Figure 11 through 2.54mm pitch dual-row 3-pin male headers. Both pins support hardware

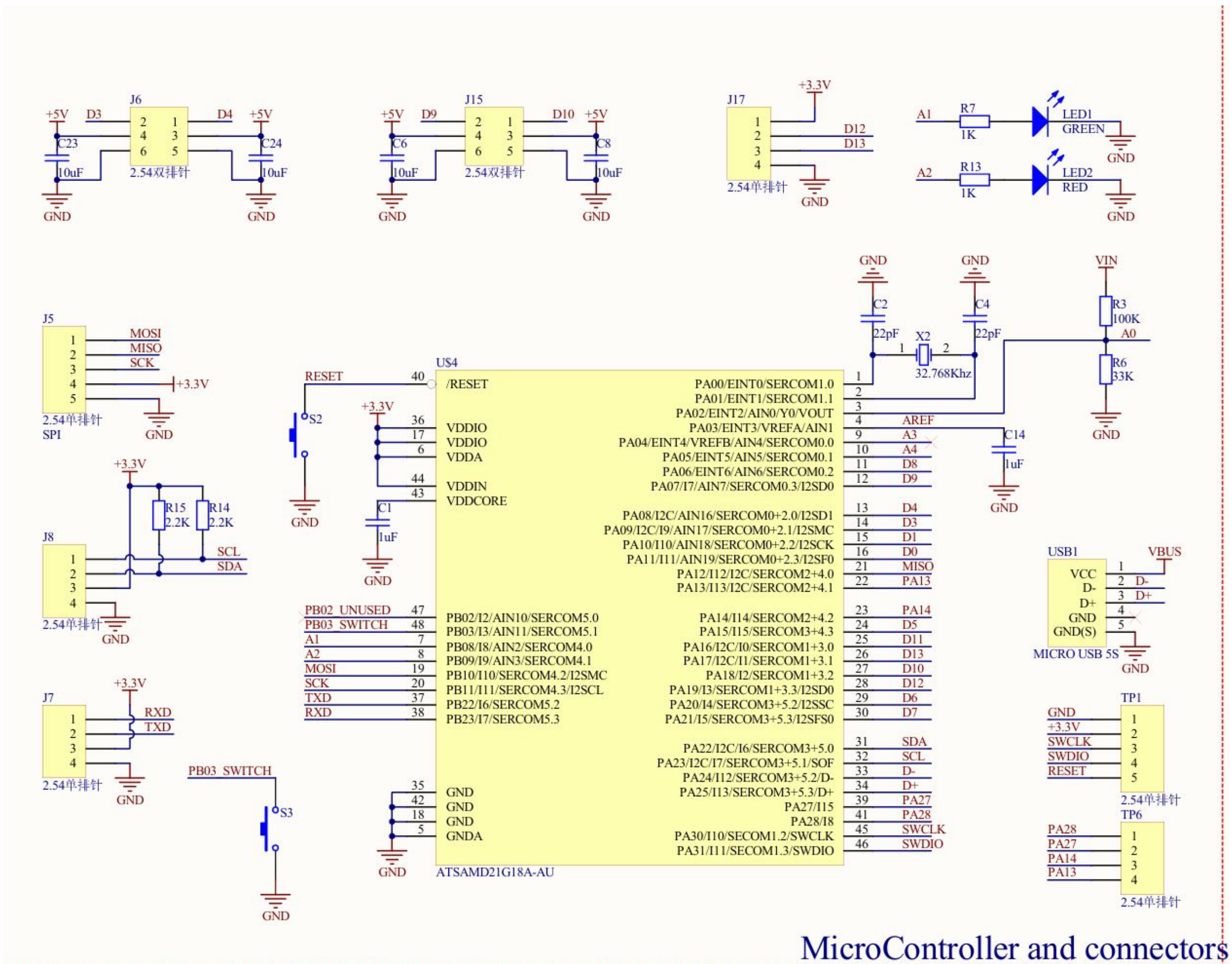


Figure 11: PCB Schematics of MicroController and Connectors

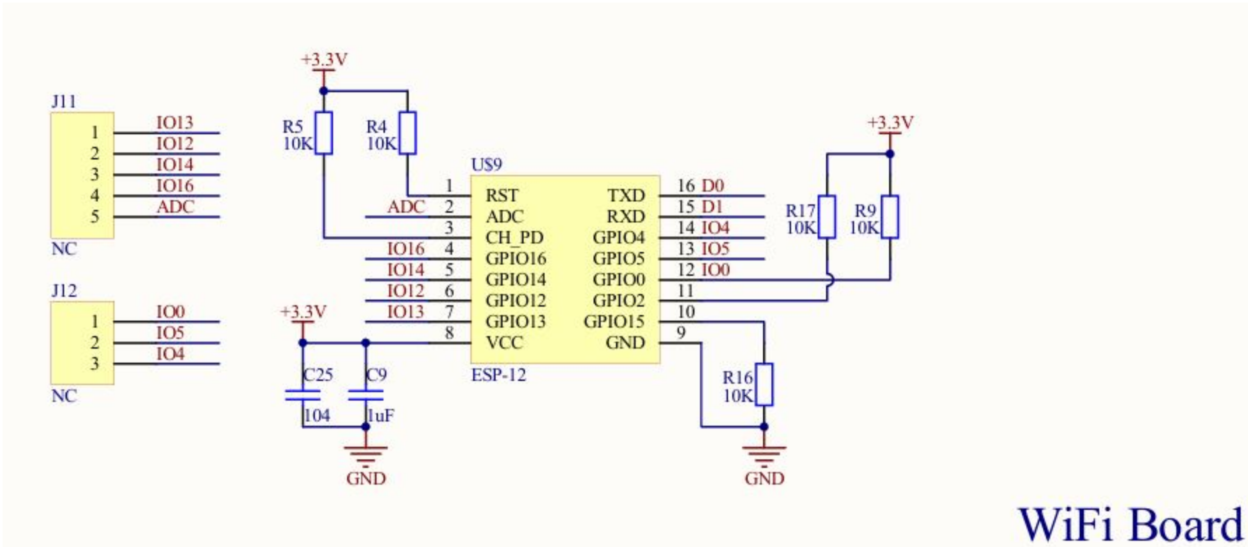


Figure 12: PCB Schematics of WiFi Board

PWM output through the TCC0 module, providing precise timing control. It could also function as general-purpose GPIO when needed, ensuring reliable mechanical connections. The 42mm*40mm NEMA 17 stepper motors are driven by dedicated motor driver modules and are connected to the chip to be activated.

We soldered 2.54mm pitch 4-pin male headers on J7, J8, J16, and J17 to give enough external extension modules. Figure11 The system integrates STMicroelectronics' VL53L5CX V2 ToF multi-zone ranging sensor (8×8 zone with a wide 65-degree diagonal FoV detection, 60 Hz refresh rate, 0-4m range via 940nm VCSEL) [3] with TDK InvenSense's ICM-42688 6-axis MEMS motion sensor (featuring ±2000 dps 3-axis gyro, ±16g 3-axis accelerometer, and on-chip DMP)[4]. These synchronized sensors will be used along with reflective stickers to enable precise robotic arm pose control.

We conserved an ESP8266 board as a WiFi board in order to realize wireless communication with the computer and controller Figure 12.

In this part, there are three sets of 2-row female headers, 8-pin per set with 2.54mm pitch, as shown in Figure 13. These plugs are prepared for three A4988 stepper motor driver modules. Three 2.54mm pitch 4-pin male headers are soldered to power and control stepper motors.

## 2.3 Pottery Wheel

The pottery wheel is used to supply stable rotational force, which helps the manipulator better control the thickness and shape of the clay in the molding process. In the process of kneading, it can accurately adjust the speed and smooth the clay wall in the process of rotation, improving the fineness and consistency of the finished product. Its key feature is a flat, level working platform that ensures the clay remains centered during rotation,

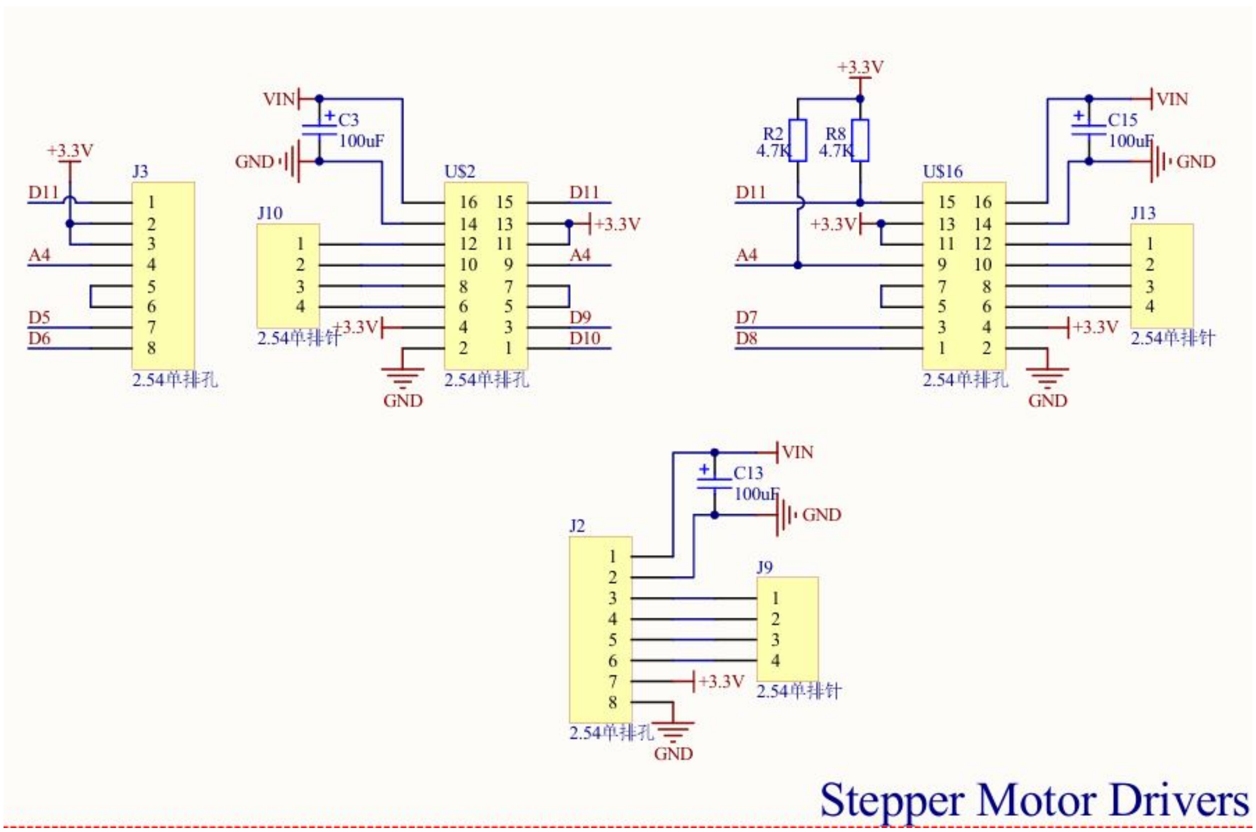


Figure 13: PCB Schematics of Stepper Motor Drivers

reducing eccentric movement and allowing for uniform shaping. By maintaining a fixed central axis, the wheel allows the manipulator to apply localized pressure on one side of the clay wall while the rotation distributes the force evenly; thus, the pulling up and shaping part is applied to all clay wall around.

Figure 14: Pottery Wheel

We use a commercially available version of a pottery wheel Figure 14. The diameter of the pottery wheel is 15cm, and there is a detachable birdbath around the wheel. The weight is 2.2kg, which provides enough stability in shaping clay products of 5cm * 5cm * 10cm. The speed can be freely adjusted from 0 to 240 RPM. Speed can decrease due to excessive downward pressure on the wheel. Considering the clay we use is around 100g and we are mainly doing pulling up jobs, so the pressure on the wheel is lighter. Only when the end effector is doing a hole-sawing job will the ball-shaped end effector apply an extra 50g to 200g of pressure, which adds up to at most 350g of downforce. This is within the scope of the work permit pressure.

To verify if the pottery wheel is suitable for shaping clay, the following image is one attempt of us trying to use this pottery wheel to hand-shape clay and it was successful in centralizing. And the RPM is enough for shaping when the moisture is suitable. The simulation is shown in Figure 15. It shows that the rotation speed and weight of this pottery wheel are sufficient to complete the task.

Figure 15: Pottery Wheel in Operation

## 2.4 Software Control

### 2.4.1 `wallshape3.py` – Wall-shape Customization Interface

The `wallshape3.py` script is the entry of the software part. In this Python script, we write a graphic user interface based on the `tkinter` framework. As shown in Figure 16, users are given a canvas, which illustrates the cross section on one side of the pottery wall with respect to the wheel axis. The height of the target pottery and the width of the half-screen could be manually assigned as a scale reference. Users are free to add control points to the external wall by double-clicking the left mouse button and to the internal wall by the right button; they can drag the control points, as well as deleting them by the middle mouse button. After clicking the `sample` button, the target wall shape will be sampled by the quadratic B-spline method; a confirmation box then pops up to ask the users whether to perform the shaping program.

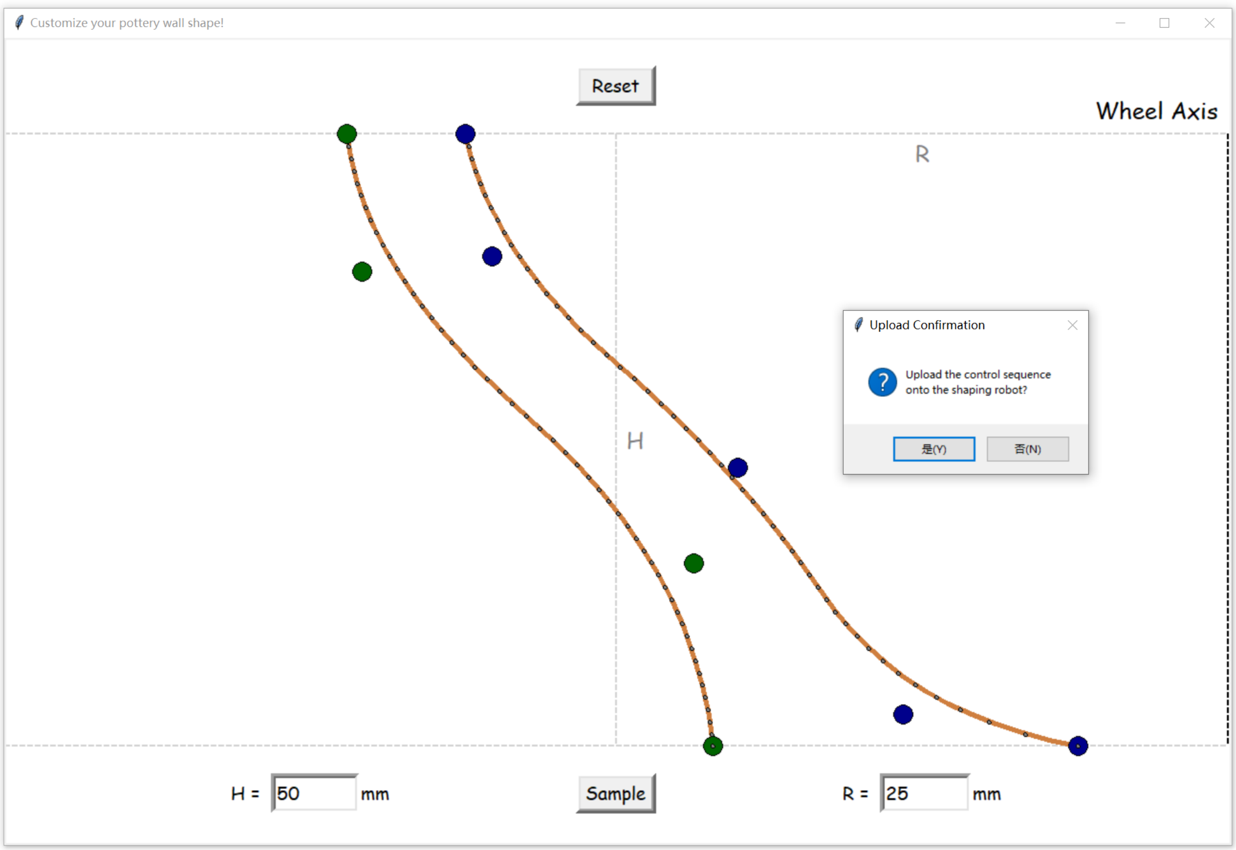


Figure 16: A Screenshot of `wallshape3.py`.

### 2.4.2 `pybotarm3.py` – Manipulator Controller

The `pybotarm3.py` script is a command mediator that bridges the high-level application layer to the microprocessor. In the Arduino driver code [1] uploaded to the microprocessor, a valid control sequence consists of an operation followed by eight `short` `int` values – for example, in `move` operation, the first five values correspond to the destination states of the motors. We write this script to further encapsulate the control behavior into a Python class, and expose the necessary interfaces, like the forward kinematic movement, by specifying the displacements and angles of the axes, as well as the inverse kinematic movement simulating the horizontal prismatic joint.

To calculate the inverse kinematics, we consider the target with zero $y$-value, which corresponds to the workspace on a radial plane of the wheel. According to Figure 17,

$$\begin{cases} q_1 = \arccos\left(\dfrac{x^2 + l_1^2 - l_2^2}{2xl_1}\right) \\ q_2 = \arccos\left(\dfrac{l_1^2 + l_2^2 - x^2}{2l_1 l_2}\right) - \pi \\ q_4 = -q_2 - q_1 \end{cases} \tag{1}$$

The elbow-up solution, which is what we currently use, can be trivially obtained by negating $q_1$ and $q_2$.

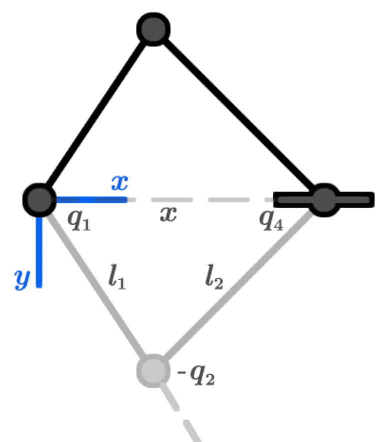


Figure 17: Inverse Kinematics on Radial Direction.

#### 2.4.3 `drivearm3.py` – Manipulator Shaping Program

The `drivearm3.py` script is the top-level software control for the motors related to customized wall shaping. This script would receive the vertical interval and the sampled trajectory of the inner and outer wall for the pottery from `wallshape3.py`. For each step in the trajectory, the script calculates an angle for the gripper to achieve the corresponding width. The angle of each gripper is calculated by:

$$q_5 = \arcsin\left(\frac{x - d + 2r}{2l}\right) \tag{2}$$

Where $x$ is the input from `wallshape3.py` indicating the desired wall radius, $d$ is the length between the two gripper axes, $r$ is the radius of the end effector, and $l$ is the length from the axis to the end effector. After having the angle $q_5$, for each step in the trajectory, `drivearm3.py` controls the end effector to maintain the width at the related height to shape the pottery from the bottom to the top, simulating the handmade process of pulling up and shaping steps.

# 3 Cost & Schedule

## 3.1 Cost

Table 1: Cost Table

| Item | Description | Quantity | Total Price (CNY) |
|---|---|---|---|
| Pottery Wheel | ⌀12.5cm, rpm 0-240, 2.2kg | 1 | 230 |
| Porcelain Clay | High-Whiteness, 400g | 24 | 54 |
| PCB | ESP32, 30Pin | 1 | 6.01 |
| Jumper Wire | sg-220, 21cm | 1 | 4.05 |
| Type-C Wire | Blue, 0.3m | 1 | 1.68 |
| PCB | ESP32-WROOM-32 | 2 | 48.14 |
| PCB | 0.96 OLED IIC | 1 | 9.17 |
| SCARA Kit | 3 NEMA 17 Stepper Motors & 3D-Printed Components | 1 | 711 |
| Jumper Wire | 21cm, M/M, M/F, F/M, F/F | 30 each | 8.39 |
| Sensor | VL53L5CX module, Optical cover, driver board | 1 | 54 |
| Sensor | ICM42688, driver board | 1 | 61.20 |
| Female header | 2.54mm pitch 4-pin | 20 | 2.40 |
| Pin header | 2.54mm pitch 4-pin | 50 | 1.32 |
| Servo motor | MG995, 180 degree tolerance | 1 | 21.14 |
| Servo motor | MG90S, 180 degree tolerance | 3 | 10.28 |
| Servo motor | DS3218, 180 degree tolerance | 1 | 58.31 |
| Multimeter | 2000 $\mu$F | 1 | 40.56 |
| Self-tapping Screw | M2*8, M2*10, M2*12, M2.3*8, M2.3*10 | 300 each | 15.96 |
| Flat head Screw | M2*10 | 100 | 1.67 |
| Stepper motor | 42mm*40mm, NEMA 17 | 2 | 19.90 |
| Reflective patch | 3M, 3cm*3cm | 10 | 8.80 |
| DC-DC converter | input 3V to 15V, output 5V | 1 | 4.58 |
| DC-DC converter | input 3V to 18V, output 6V | 1 | 7.80 |

### 3.2 Schedule

Table 2: Schedule

| **Week** | **Shihan Lin** | **Zixu Zhu** | **Mofei Li** | **Minhao Shi** |
|---|---|---|---|---|
| 4.14 – 4.20 | Design End Effector | Assemble Manipulator | Learn Arduino | 3D print End Effector |
| 4.21 – 4.27 | Complete software architecture | Test Arduino performance | Test and compare Arduino performance | Test and compare Arduino performance |
| 4.28 – 5.04 | Build Final overall system | Writing code on wall shaping | Build Final overall system | Build Final overall system |
| 5.05 – 5.11 | Collect Data and visualization | Document Data; Final debug | Final Debug | Final Debug |
| 5.12 – 5.18 | Prepare Final Presentation | Prepare Final Presentation | Prepare Final Presentation | Prepare Final Presentation |
| 5.19 – 5.26 | Complete Final Report | Complete Final Report | Complete Final Report | Complete Final Report |

# 4 Requirements & Verification

## 4.1 Completeness of Requirements

### 4.1.1 Software Control Requirements

For the theoretical accuracy, a resolution under $0.1(mm)$ for the wall shaping is required for software control. This requires users to be able to customize their product under the precision of $0.1(mm)$ at the GUI.

Owing to constraints in budget and materials, the allowable deviation in shaping width during manipulation is set to $3\,\text{mm}$, with a tolerance of approximately $\pm 1\,\text{mm}$.

### 4.1.2 Manipulator Requirements

The manipulator should be able to control its positioning accuracy within a 1 mm error margin relative to the target location. Its movements must be repeatable and able to transition from the current position to the target position in the most efficient manner. The motion should be smooth, without prolonged lag, and should not produce vibrations exceeding 3 mm in amplitude. Additionally, during movement, the manipulator must avoid any contact with the clay.

## 4.2 Appropriate Verification Procedures

### 4.2.1 Verification Procedures for Power Supply and motors

The LED on the PCB should turn red and keep illuminating after plugging in the micro usb to the board. The LED should turn white from red after plugging in the AC/DC adapter. Verification for motors is combined with the following verification for software control.

### 4.2.2 Verification Procedures for the Software Control

The accuracy of software control can be checked from the command sets sent to the robotic manipulator. For more details, please refer to the next section.

### 4.2.3 Verification Procedures for Wall Shaping Requirements

Measuring the width of the shaped pottery at several key points using a caliper and comparing it with the input profile. Ensure that all measurements are within a $1$ mm tolerance.

### 4.2.4 Verification Procedures for Manipulator

The manipulator executes the same trajectory multiple times, and the end-effector position deviation is recorded (standard deviation should be $\leq$ 1 mm). Acceleration sensors are used to measure vibration amplitude (ensuring it remains $\leq 3$ mm). The manipulator operates in an actual working environment, maintaining stable performance without actively colliding with obstacles.

## 4.3 Quantitative Results

### 4.3.1 Quantitative Results for the Software Control

The minimum

$$\text{Unit Degree} = \frac{9 \times \text{Interval of Pulse Width}}{10^5}\,^{\circ} \tag{3}$$

*Unit Degree* denotes the smallest angular increment by which the servomotor can rotate in a single step. Considering the length between the end effector and the gripper axis is far larger than the unit width, we could use this approximation:

$$\text{Unit Width} = L \tan(0.036^{\circ}) \tag{4}$$

*L* denotes the length between the end effector and the gripper axis, $0.036^{\circ}$ is the degree we get from the last step. For the current model, $L = 120(mm)$, which gives us a resolution of $0.0754(mm)$. This is under the tolerance.

# 5 Conclusion

## 5.1 Accomplishments

### 5.1.1 Automated Shaping

The robot arm based on the SCARA kit successfully implements the most steps in the pottery production: centering, pulling up, and shaping. The manipulator can achieve high accuracy controlling the trajectory tracking, ensuring the integrity of the clay produced and the symmetry and high consistency of the pottery wall.

### 5.1.2 User Customization

We created a beautiful and easy-to-use graphical interface that allows users to create and move distortion points. Based on these points, the program uses quadratic B-spline sampling to plan the trajectory of the inner and outer walls of the clay, which is highly customizable and convenient. Secondly, the program samples the trajectory and sends the running trajectory to the motor driver through the driver program for high-precision control. At the same time, the sampling frequency can be adjusted by the user, which further improves the accuracy of the control.

## 5.2 Uncertainties

### 5.2.1 Errors Caused by Vibration

The systematic error caused by vibration is a link that cannot be ignored. The vibration of the robot arm causes the actual position of the end to shake. The causes of vibration are as follows:

- Motor start-stop impact and inertia: The instantaneous torque changes generated by the stepper motor and servo during rapid start-stop or acceleration and deceleration
- Connection structure: 3D-printed parts cannot achieve very high-precision coupling, so there is room for shaking in connection parts such as transmission belts. At the same time, the larger torque in the mechanical design amplifies this disadvantage.

### 5.2.2 Clay Accumulation

The end-effector used to shape clay will touch with the clay during the working process. In order to make the clay shapeable, increasing the moisture content of the clay is necessary. However, this will also increase the viscosity of the clay, which results in a layer of clay ”shell” forming on the end-effector after working, and the actual contact with the clay is no longer the designed end-effector but this ”shell”. The increase in thickness and shape uncertainty at the contact position significantly increases the error of the final shaping result.

## 5.3 Future Work/Alternatives

### 5.3.1 Closed-loop Control

To improve the accuracy of clay centering and closed-loop control in the automated pottery wheel system, we plan to use a solution that integrates a VL53L5CX laser sensor and an upgraded gyroscope. The VL53L5CX, mounted vertically above the end effector, will use its 8x8 range finding matrix (4mm resolution) to provide a real-time 3D surface profile of the clay and locate the center of mass of the clay. The gyroscope mounted on the end effector will collect motion data. These sensors will feed into a PID control architecture: the outer loop adjusts the trajectory of the robot based on the laser-derived center of mass data, while the inner loop uses gyroscope feedback to correct the joint angles.

### 5.3.2 Counterweight Base

To improve the stability of the robot arm during high-speed movements or heavy-load operations, a balancing base will be integrated into the system. This lowers the center of gravity of the system, reduces vibrations, and minimizes tilting during dynamic movements. Slippery rubber pads should also be added to ensure a secure connection to the workbench. This upgrade ensures precise positioning while maintaining operational safety.

## 5.4 Ethical Risk

### 5.4.1 Unconscious Plagiarism

We refer to technology documents and modify some existing publicly available mechanical structures to meet our needs. We believe that all of our team members are honest and respect the intellectual property of others, but we must be careful about the risk of unintentional plagiarism. Therefore, we must confirm the similarity between our code and the references and assess whether the copyright of the mechanical structure can be used.
(AMC code of ethics: 1.5 Respect the work required to produce new ideas, inventions, creative works, and computing artifacts.)

### 5.4.2 Safety first

During any experiment and test, we promise that we will take safety as the most important principle. Any behavior that may put members or other people in danger will be completely ruled out.

### 5.4.3 Protect the environment and reduce waste

To obey the IEEE code for Ethics [5], we promise not to use materials that are extremely harmful to the environment during the experiment. During the experiment, we will try to reuse the clay used for the experiment as much as possible and reduce the waste of electricity and water.

### 5.4.4 Honest

We will honestly admit our mistakes and sincerely accept the advice of others. At the same time, no form of cheating is allowed. If we receive guidance from previous works, we will indicate the source in the quotation.

### 5.4.5 Professional

During the work process, we will strive to achieve high quality of project design. During the project process, we should conduct a comprehensive and thorough assessment of the skills required for the project and only work within our capabilities. At the same time, we should strive to improve our professional skills and maintain high standards of professional ability.

### 5.4.6 Teamwork

During the project, we promise to respect everyone fairly and not discriminate against others based on the task. We will not participate in any form of harassment or insults, and everyone's ideas will be respected. In the process of group cooperation, while every member should do the work they are good at, each member should be given the space to exert their abilities.

# References


[1] jjrobots. "Scara robotic arm by jjrobots." (2019), [Online]. Available: https://sketchfab.com/3d-models/scara-robotic-arm-by-jjrobots-6db379cb0c064c2e8d0e7fd01469bf44 (visited on 04/14/2025).

[2] T. Inc. "Servos & parts - TowerPro rc model products." (2023), [Online]. Available: https://towerpro.com.tw/product-category/servos-parts/ (visited on 05/10/2025).

[3] STMicroelectronics. "VL53L5CX - time-of-flight 8×8 multizone ranging sensor with wide field of view." (Jun. 2023), [Online]. Available: https://www.st.com/en/imaging-and-photonics-solutions/vl53l5cx.html.

[4] TDK InvenSense. "ICM-42688-P - 6-axis mems motion sensor with dmp." (Jul. 2021), [Online]. Available: https://invensense.tdk.com/products/motion-tracking/6-axis/icm-42688-p/.

[5] IEEE. "IEEE Code of Ethics." (2016), [Online]. Available: https://www.ieee.org/about/corporate/governance/p7-8.html (visited on 02/08/2020).